# 14-3-3σ Modulates Pancreatic Cancer Cell Survival and Invasiveness

Divas Neupane and Murray Korc

**Abstract**

**Purpose:** The purpose of the present study was to investigate the potential role of 14-3-3σ in pancreatic ductal adenocarcinoma (PDAC).

**Experimental Design:** 14-3-3 isoform expression was determined by real-time quantitative PCR in laser capture normal pancreatic ductal cells and pancreatic cancer cells and in 5 pancreatic cancer cell lines. PANC-1 cells, with low levels of 14-3-3σ, were stably transfected with a human 14-3-3σ cDNA. Conversely, high endogenous 14-3-3σ levels in T3M4 cells were suppressed by specific short hairpin RNA. Apoptosis, motility, and invasiveness were studied.

**Results:** The cancer cells in 7 PDAC samples expressed high levels of 14-3-3σ mRNA by quantitative PCR when compared with normal pancreatic duct cells. 14-3-3σ protein levels were high in BxPC3, COLO-357, and T3M4 cells, intermediate in ASPC-1 cells, and low in PANC-1 cells. Most cell lines released detectable amount of 14-3-3σ into conditioned medium. Overexpression of 14-3-3σ in PANC-1 cells led to resistance to cisplatinum-induced apoptosis, increased basal migration, and increased invasion in response to epidermal growth factor and insulin-like growth factor-I. By contrast, short hairpin RNA-mediated knockdown of endogenous 14-3-3σ in T3M4 cells did not alter migration but led to enhanced cisplatinum sensitivity, increased invasiveness in response to epidermal growth factor, and decreased invasiveness in response to insulin-like growth factor-I.

**Conclusions:** 14-3-3σ contributes to the chemoresistance of pancreatic cancer cells and exerts cell type-dependent effects on cell migration and invasion. Therefore, strategies aimed at suppressing 14-3-3σ expression and function may have a therapeutic benefit in subgroups of patients with PDAC.

Pancreatic ductal adenocarcinoma (PDAC) is the fourth leading cause of cancer mortality in the United States, with a 5-year survival rate that remains <5% (1). Although our understanding of the molecular and genetic basis for this disorder is expanding, there has only been modest progress in its treatment. There is a high frequency of *K-ras*, *p53*, *p16*, and *Smad4* mutations in PDAC in conjunction with overexpression of tyrosine kinase receptors and their ligands and excessive activation of mitogenic signaling pathways (2, 3). Moreover, the cancer cells in PDAC exhibit apoptosis resistance. The mechanisms that underlie this increased resistance to apoptosis-inducing signals have not been completely elucidated but have been attributed to constitutive nuclear factor-κB and Akt activation, altered expression of antiapoptotic proteins such as Bcl-2, Bcl-$X_L$, and the inhibitor of apoptosis proteins, and increased Smad7 and thioredoxin expression (4, 5).

**Authors' Affiliation:** Departments of Medicine and Pharmacology and Toxicology, Dartmouth-Hitchcock Medical Center and Dartmouth Medical School, Hanover, New Hamsphire

Received 5/28/08; revised 7/16/08; accepted 8/6/08.

**Grant support:** USPHS grant CA-10130 (M. Korc).

The costs of publication of this article were defrayed in part by the payment of page charges. This article must therefore be hereby marked *advertisement* in accordance with 18 U.S.C. Section 1734 solely to indicate this fact.

**Requests for reprints:** Murray Korc, Departments of Medicine and Pharmacology and Toxicology, Dartmouth-Hitchcock Medical Center and Dartmouth Medical School, One Medical Center Drive, Lebanon, NH 03756. Phone: 603-650-7936; Fax: 603-650-6122; E-mail: murray.korc@dartmouth.edu.



doi:10.1158/1078-0432.CCR-08-1366

The 14-3-3 family consists of small (28-33 kDa) acidic proteins with evolutionarily conserved amino acid sequences that participate in the regulation of cell proliferation and survival. There are seven distinct mammalian isoforms of 14-3-3 (β, ε,γ, η, σ, θ/τ, and ζ), which often form heterodimers or homodimers and bind to >100 different proteins (6, 7). Most commonly, 14-3-3 proteins bind to target proteins possessing phosphoserine and phosphothreonine motifs (RSxpSxP or RxY/FxpSxP, where x denotes any amino acid and pS represents a phosphorylated serine; refs. 7, 8). In addition, some 14-3-3-binding partners exhibit variations from these motifs, and others lack these motifs and bind to 14-3-3 in a phosphorylation-independent manner (9).

The expression of 14-3-3σ, which is also known as human mammary epithelial marker 1 or stratifin, is mostly restricted to epithelial cells and is known to be altered in several human cancers (9). 14-3-3σ is down-regulated in many human cancers, where it has been proposed to function as a tumor suppressor gene. In breast cancer and hepatocellular carcinoma, for instance, 14-3-3σ levels are significantly decreased principally due to silencing of the gene through hypermethylation (10, 11). By contrast, 14-3-3σ expression is increased in PDAC (12–15) as well as in other cancers, such as colon carcinoma and head and neck squamous cell carcinomas (16, 17). However, the biological role of the elevated expression of 14-3-3σ in any human cancer is not known.

In the present study, we sought to delineate the potential role of 14-3-3σ in PDAC. In PANC-1 cells, which express low endogenous levels of 14-3-3σ, clones engineered to express

high levels of 14-3-3σ exhibited increased survival in the presence of cisplatinum, attenuated activation of proapoptotic pathways, enhanced basal migration, and enhanced invasiveness in response to epidermal growth factor (EGF) and insulin-like growth factor-I (IGF-I). Conversely, down-regulation of 14-3-3σ in T3M4 cells, which have high endogenous levels of 14-3-3σ, rendered the cells more sensitive to cisplatinum-induced apoptosis, did not have any effect on either basal or EGF-stimulated cell migration, but led to increased invasion in response to EGF and decreased invasion in response to IGF-I. These findings indicate that 14-3-3σ confers a survival advantage to pancreatic cancer cells that promotes their chemoresistance but exerts complex and cell specific effects on cell migration and invasion.

## Materials and Methods

***Cell culture.*** Human pancreatic cancer cell lines ASPC-1, PANC-1, and BxPC3 were purchased from the American Type Culture Collection. COLO-357 and T3M4 human pancreatic cancer cell lines were a gift from R.S. Metzgar (Duke University). ASPC-1, BxPC3, and T3M4 cells were grown in RPMI, and PANC-1 and COLO-357 were grown in DMEM (Mediatech) both supplemented with 7.5% to 10% fetal bovine serum (Omega Scientific). Cells were cultured at 37°C in humidified air with 5% $CO_2$. Serum-free medium used in this study refers to DMEM or RPMI supplemented with 0.1% bovine serum albumin, 5 μg/mL apotransferrin, and 5 ng/mL sodium selenite.

***Immunoblotting.*** Immunoblotting was done as described previously (18). For the analysis of secreted 14-3-3σ protein, RPMI or DMEM supplemented with 0.05% fetal bovine serum, 5 μg/mL apotransferrin, and 5 ng/mL sodium selenite, referred to as conditioned medium, was used. Conditioned medium was collected 48 h after feeding the cells. Protease inhibitor cocktail (Roche) was added to the collected medium, and medium was concentrated using Ultracel YM-10 membrane filter column (Millipore). The antibodies used in the studies were anti-14-3-3σ that were either rabbit polyclonal (Immuno-Biological Laboratories) or mouse monoclonal (Neomarkers); rabbit polyclonal against 14-3-3η (Immuno-Biological Laboratories); rabbit polyclonal against 14-3-3β (C-20), 14-3-3ε (T-16), 14-3-3γ (C-16), 14-3-3θ (C-17), 14-3-3ζ (C-16), and ERK-2 (C-14; Santa Cruz Biotechnology); and rat monoclonal anti-tubulin (Abcam).

***Immunohistochemistry.*** Sections (8 μm) of normal and pancreatic cancer tissue were cut from paraffin-embedded tissue. The normal tissues were obtained from an organ donor program, and the cancer tissues were obtained following surgical resection of PDAC. Slides were deparaffinized and rehydrated. The intrinsic peroxidase was blocked with 0.3% $H_2O_2$ in methanol for 30 min. Antigen demasking was done in 10 μmol/L sodium citrate buffer (pH 6.0) by heating to near boiling in microwave and then slowly cooling down to 23°C. Slides were blocked with 5% goat serum in PBS for 30 min. Then, tissue sections were incubated in 14-3-3σ antibody diluted with 5% goat serum overnight in the cold room. Sections were then incubated for 30 min in biotinylated secondary antibody from Vectastatin Universal kit (Vector Laboratories). Finally, sections were incubated in Vectastatin ABC Reagent and stained with DAB and lightly counterstained with hematoxylin. Staining in the absence of the primary antibody served as a negative control and did not yield any signal.

***Laser capture.*** Tissue specimens were obtained from 7 PDAC samples and 3 normal human pancreatic samples. The use of human tissue samples was approved by the Human Subjects Committee at Dartmouth Medical School. Laser capture microdissection on these samples was carried out as described previously from our laboratory (19). Briefly, tissue cryosections (6-8 μm) were quickly fixed in 75% ethanol and stained with 1.5% eosin Y (Sigma). Slides were air dried after dehydration in ethanol and incubation in xylene and subjected to laser capture microdissection using the Pix Cell instrument and CapSure LCM Caps (Arcturus Engineering).

***Reverse transcription and real-time quantitative PCR.*** Total RNA from each laser capture tissue sample was isolated using Absolutely RNA Nanoprep or Strataprep Total RNA Microprep kit (Stratagene). The concentration of RNA was determined by using RiboGreen (Molecular Probes) and a CytoFluor florescence plate reader (Per-Septive Biosystems). RNA (20 ng) was reverse transcribed using Sensiscript RT kit (Qiagen). For studies in cell lines, total RNA was extracted by the acid guanidinium thiocyanate-phenol-chloroform method (20). Integrity of RNA was assessed by running on a 1% agarose gel, staining with ethidium bromide, and visualizing under UV light. RNA was reverse transcribed using random hexamer primers and the SuperScript kit (Invitrogen) according to the manufacturer's protocol. For both tissue and cell line studies, 50 cycles of quantitative real-time PCR was done in a 7700 Sequence Detector from Applied Biosystems. Primers and probe sets were designed using Primer Express 1.5 software (Applied Biosystems). Primers and probes were verified for specificity by individually blasting them against the National Center for Biotechnology Information database and custom ordered from Qiagen. The following sequences were used for the primers and probes: 14-3-3β forward AAGAGAGAAATCTGCTCTCTGTTGC, 14-3-3β reverse GGAGATGACACGCCAGGAAG, and 14-3-3β probe 6-FAM-ACAAGAATGTGGTAGGCGCCCGC-TAMRA; 14-3-3ε forward ATGGATGATCGAGAGGATCTGG, 14-3-3ε reverse CTCCACCATTTCGTCGTATCG, and 14-3-3ε probe 6-FAM-CAGGCGAAGCTGGCCGAGCA-TAMRA; 14-3-3γ forward CGTGCGTACCGGGAGAAG, 14-3-3γ reverse TCCAGCAGGCTCAGCACA, and 14-3-3γ probe 6-FAM-AGAGAAGGAGTTGGAGGCTGTGTGCCA-TAMRA; 14-3-3η forward TGGTGCCAGGCGATCTTC, 14-3-3η reverse TCGTTTCCATCAGCCATGG, and 14-3-3η probe 6-FAM-TGGAGGGTCATTAGCAGCATTGAGCAG-TAMRA; 14-3-3σ forward CAGTCTGATCCAGAAGGCCAA, 14-3-3σ reverse GAAGGCTGCCATGTCCTCA, and 14-3-3σ probe 6-FAM-TGGCAGAGCAGGCCGAACGC-TAMRA; 14-3-3θ forward CGCCTGGAGGGTCATCTCTA, 14-3-3θ reverse TCCTTAATCAGCTGCAACTTCTTG, and 14-3-3θ probe 6-FAM-TCGAGCAGAAGACCGACACCTCCG-TAMRA; and 14-3-3ζ forward GAGCAAGGAGCTGAATTATCC, 14-3-3ζ reverse GACCTACGGGCTCCTACAAC, and 14-3-3ζ probe 6-FAM-TGAGGAGAGGAATCTTCTCTCAGTTGCT-TAMRA.

***Cloning of full-length human 14-3-3σ and generation of stable clones.*** Total RNA from BxPC3 was reverse transcribed using random hexamer primers as described above, and 14-3-3σ cDNA was amplified by PCR using the following primers: forward ATAAGCTTCCAGAGCCATGGAGA and reverse CACGTGGCTCTGGGGCTCCTG. The PCR-amplified gene product was cloned into TOPO-TA cloning vector (Invitrogen). The gene was cloned in the *Hin*dIII/*Bbr*pI sites of the pMH vector (Roche Biochemicals), which encodes a COOH-terminal hemagglutinin antigen (HA) epitope tag in frame with the gene (construct named pMH-14-3-3σ-HA). PANC-1 cells were stably transfected with pMH-14-3-3σ-HA. The stable clones were selected in complete DMEM supplemented with 800 μg/mL geneticin (Life Technologies). Two clones expressing similar levels of 14-3-3σ were chosen for subsequent experiments.

***Immunocytofluorescence.*** PANC-1 sham- and 14-3-3σ-transfected clones ($1.5 \times 10^5$) were seeded on LabTek chamber slides (Nalge Nunc) and incubated at 37°C for 48 h, washed with PBS, and fixed in 2% paraformaldehyde for 10 min. Cells were washed extensively with PBS, incubated for 10 min with 50 mmol/L $NH_4Cl$ in PBS, and permeabilized/blocked with 0.1% Triton X-100/PBS-2% bovine serum albumin for 15 min (21). Cells were then incubated for 1 h at 23°C with anti-14-3-3σ antibody, washed with PBS, and then incubated with Alexa Fluor 488 goat anti-mouse secondary antibody (Invitrogen) for 30 min at 23°C. Finally, cells were counterstained with Hoechst 33258 (0.5 mL of 0.2 μg/mL stock) for 5 min. Cells were examined using Olympus BX60 upright microscope (Olympus) fitted with Olympus DP 70 camera, and pictures were taken using Image-Pro Plus software (Media Cybernetics).

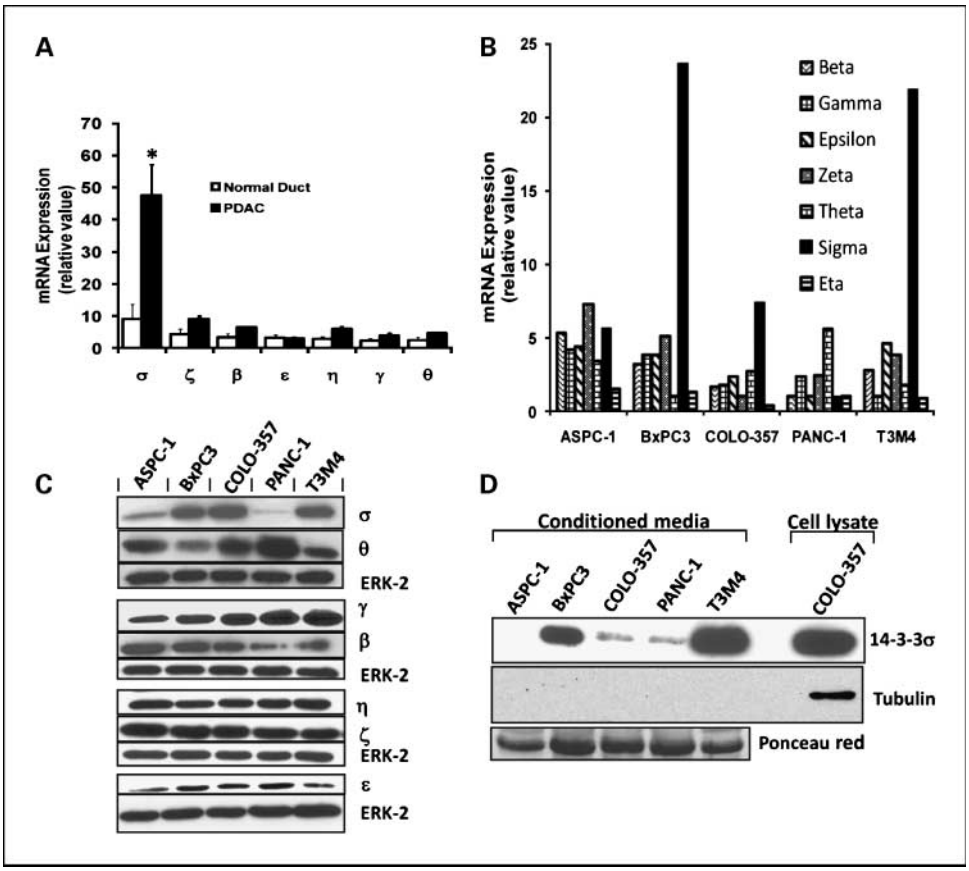


**Fig. 1.** Expression of 14-3-3 isoforms in pancreatic tissue and pancreatic cancer cell lines. *A,* 14-3-3 mRNA expression in laser capture pancreatic tissue. RNA isolated from laser capture normal ductal cells from 3 normal pancreas and cancer cells from 7 PDAC samples were subjected to real-time quantitative PCR using isoform specific primers and probes. Mean ± SE. *, $P < 0.03$, compared with values obtained in normal ducts or with values in the cancer cells for the other members of the 14-3-3 family. *B,* 14-3-3 mRNA expression in pancreatic cancer cell lines. Total RNA isolated from the indicated cells lines was reverse transcribed and subjected to real-time PCR as described in Materials and Methods. Results were normalized to 18S levels. Mean of two independent experiments done in duplicate in which similar results were obtained. *C,* expression of 14-3-3 proteins in pancreatic cancer cell lines. Whole-cell protein lysates (20 μg/lane) were subjected to immunoblotting with antibodies specific for the indicated 14-3-3 isoform. Membranes were stripped and probed for ERK-2 to verify equal protein loading. *D,* secretion of 14-3-3σ. Protein concentrates from conditioned medium (40 μg/lane) were prepared from the indicated cell lines and subjected to immunoblotting with the anti-14-3-3σ antibody. Whole-cell lysate from COLO-357 cells (20 μg) served as a positive control. The membrane was blotted for tubulin to ensure that cytoplasmic proteins were not being spuriously released in conditioned medium. The membrane was also stained with Ponceau red to verify equal loading of lanes.

***3-(4,5-Dimethylthiazol-2-yl)-2,5-diphenyltetrazolium bromide assay.*** Sham-transfected PANC-1 cells and 14-3-3σ-transfected clones ($1 \times 10^4$) were plated in 96-well plates (6 wells per sample). Cells were allowed to attach and grow for 48 h in complete medium and then treated with complete medium in the absence or presence of 10 μg/mL cisplatinum (Sigma) for 48 h followed by the addition of 3-(4,5-dimethylthiazol-2-yl)-2,5-diphenyltetrazolium bromide (Sigma) at a final concentration 0.55 μg/mL. After an additional 4 h incubation, absorbance at 570 nm was determined, with a reference of 650 nm, using a Emax precision microplate reader (Molecular Devices) as reported previously (5). We have determined previously that in pancreatic cancer cell lines the 3-(4,5-dimethylthiazol-2-yl)-2,5-diphenyltetrazolium bromide assay correlates closely with cell growth as determined by cell counting and by assessing [$^3$H]thymidine incorporation (22, 23).

***Cisplatinum-induced apoptosis.*** Sham- or 14-3-3σ-transfected PANC-1 cells were incubated for 24 h in complete medium in the absence or presence of 10 μg/mL cisplatinum. Scrambled or 14-3-3σ-specific short hairpin RNA (shRNA)-infected T3M4 cells were incubated in complete medium for 24 h that was supplemented with 10 μg/mL cisplatinum for the initial 2 or 6 h or the entire 24 h. Both floating and adherent cells were then collected and lysed in the buffer containing protease inhibitors, subjected to 10% SDS-PAGE, and immunoblotted with specific antibodies against cleaved poly(ADP-ribose) polymerase (PARP) and cleaved caspase-3 (Cell Signaling Technology) as reported previously (5).

***Cell migration assay.*** To assess the motility properties, *in vitro* wound-healing assay or migration assays were done. Cells were grown to confluence in 6-well tissue culture plates and serum starved overnight, and the monolayer was scratched with a 200 μL pipette tip generating two parallel wounds. The scratched wells were washed to remove cell debris and incubated for next 24 h in serum-free medium in the absence or presence 1 nmol/L EGF with or without the Src family kinase inhibitor 4-amino-5-(4-chlorophenyl)-7-(*t*-butyl)pyrazolo[3,4-*d*]pyrimidine (PP2; Alexis). To monitor cell migration, photographs were taken of each well at five marked locations under ×40 magnification immediately after wounding (t0) and again 24 h after wounding (t24) using an inverted microscope fitted with a digital camera (Nikon Diaphot 300). The wound area of five matched pictures at t0 and t24 from each well were then measured using the ImageJ software (NIH), and the percentage change in the wound area was calculated.

***Cell invasion assay.*** Cell invasion was measured as reported previously, with some modification (24). Briefly, cells were suspended in 500 μL serum-free medium (0.1% bovine serum albumin) and placed onto the upper compartment of Matrigel-coated Transwell chambers (8 μm pore size, BioCoat Matrigel Invasion Chambers; BD Biosciences). The lower compartment was filled with 750 μL medium containing serum-free medium in the absence or presence of the respective growth factors. After 18 to 20 h, cells on the upper surface of the filter were carefully removed with a cotton swab and the membranes were fixed in methanol. The cells that had migrated through the membrane to the lower surface of the filter were stained with toluidine blue (Fisher Scientific) and counted using a light microscope.

***Down-regulation of 14-3-3σ by shRNA using lentivirus gene delivery system.*** Two different shRNA oligo sequences targeting 14-3-3σ (GenBank accession no. NM_006142) were designed based on small interfering RNA sequences (italicized) against 14-3-3σ (Dharmacon): sh1 sense T*CGAGACAACCTGACACTGT*TTCAAGAGAACAGTGT-TCAGGTTGTCTCGTTTTTTC and sh1 antisense TCGAGAAAAAACGA-GACAACCTGACACTGTTCTCTTGAAACAGTGTCAGGTTGTCTCGA and sh2 sense T*GGAGAGAGCCAGTCTGATC*TTCAAGAGAGATCA-AGACTGGCTCTCTCCTTTTTTc and sh2 antisense TCGAGAAAAAAGG-AGAGAGCCAGTCTGATCTCTCTTGAAGATCAGACT GGCTCTCTCCA.

The control shRNA was designed not to target any known mammalian gene by scrambling small interfering RNA sequence used

in sh2 (italicized): shCtrl sense T*ACGAGCGAGGTGCCGATAT*TTCAAAGAGAATATCGGCACCTCGCTCGTTTTTTTC and shCtrl antisense TCGAGAAAAAAACGAGCGAGGTGCCGATATTCTCTTGAAATATCGGCACCTCGCTCGTA.

The sense and antisense oligonucleotide templates (Sigma Genosys) were annealed together and cloned in the *Xho*I/*Hpa*I sites of the pLentiLox 3.7 lentiviral vector (Addgene). Lentivirus particles were produced by four plasmid transfection system as follows. 293T cells were transfected with 60 μg shRNA lentiviral vector construct and 30 μg each of the helper plasmids (VSVG, pRSV-Rev, and pMDLg/pRRE; all from Addgene). The supernatant containing the virus particles was collected at 48 and 72 h post-transfection and concentrated using an ultracentrifuge at 25,000 rpm for 1.5 h. The pellets were suspended in 25 μL Opti-MEM (Invitrogen) overnight and pooled together, and supernatants were aliquoted. Viral titer was determined by generating a 10-fold dilution series and infecting 293T cells ($1 \times 10^5$ per well) in a 6-well plate and by analyzing the percent enhanced green fluorescence protein-positive cells by flow cytometry at 72 h after infection. T3M4 cells were infected at a multiplicity of infection of 40 and the knockdown of 14-3-3σ was confirmed by Western blotting and quantitative PCR.

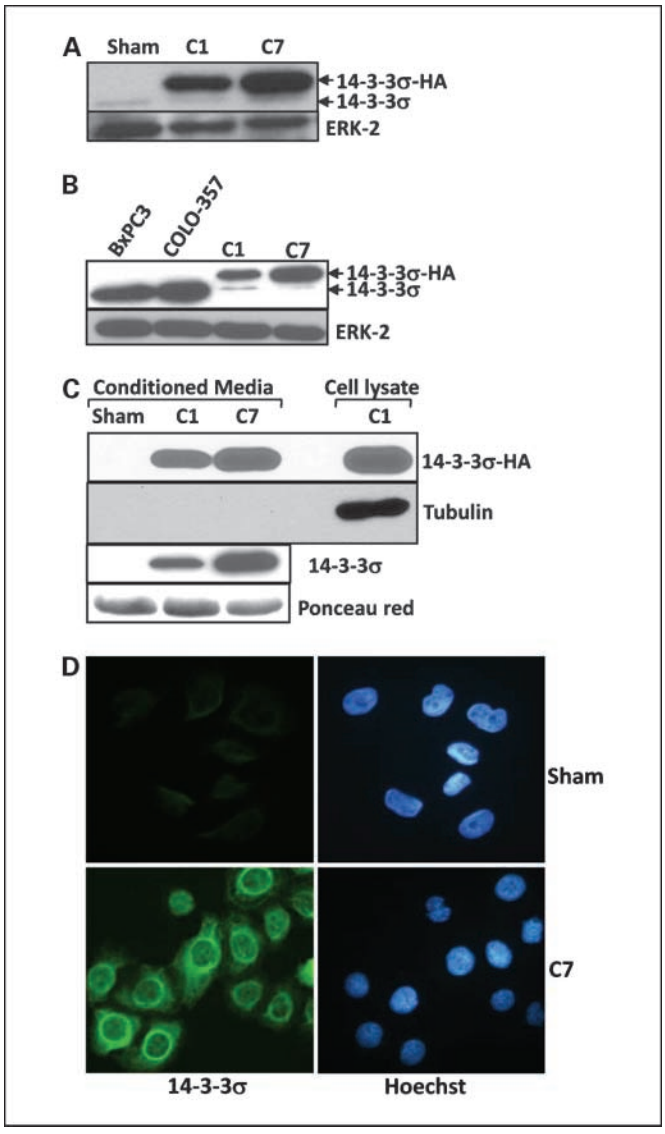


**Fig. 2.** Engineered overexpression of 14-3-3σ. *A,* PANC-1 cells were stably transfected with an empty vector (Sham) or with the full-length human 14-3-3σ cDNA that was tagged with HA, yielding clone 1 (C1) and clone 7 (C7). Cell lysates (20 μg/lane) from sham and clones were probed with the anti-14-3-3σ antibody. *B,* comparison of 14-3-3σ levels in PANC-1 clones C1 and C7 with the levels of 14-3-3σ expressed in parental BxPC3 and COLO-357 cells (20 μg/lane). *A* and *B,* HA-tagged 14-3-3σ protein is slightly shifted (*top band*) compared with endogenous 14-3-3σ (*bottom band*). ERK-2 served as a loading control. *C,* levels of secreted 14-3-3σ in conditioned medium. Protein concentrates from conditioned medium (40 μg/lane) were subjected to immunoblotting with anti-HA and anti-14-3-3σ antibody. Whole-cell protein lysate from C1 was used as a positive control for the detection of HA-tagged 14-3-3σ protein in conditioned medium. The membrane was blotted for tubulin to ensure that cytoplasmic proteins were not being spuriously released in conditioned medium. The membrane was also stained with Ponceau red to verify equal loading of lanes. *D,* localization of 14-3-3σ protein. Immunofluorescent staining of sham-transfected (Sham) and 14-3-3σ-transfected PANC-1 cells (C7) was done with the anti-14-3-3σ antibody. Hoechst staining was used to visualize the nuclei. Representative of two independent experiments, with similar staining patterns observed in both experiments. Magnification, ×400.

## Results

***Analysis of 14-3-3 expression in human pancreatic tissue and pancreatic cancer cell lines.*** The expression of all seven 14-3-3 isoforms was determined in RNA prepared from laser capture normal pancreatic duct cells and pancreatic cancer cells. We found that, among all the 14-3-3 isoforms expressed in the laser capture cancer cells, 14-3-3σ mRNA levels were the highest. Moreover, 14-3-3σ mRNA levels were increased 5-fold in cancer cells in comparison with the corresponding levels in RNA isolated from laser capture normal ductal cells (Fig. 1A). All seven tested samples exhibited increased 14-3-3σ immunoreactivity in the cancer cells within the PDAC samples (data not shown).

Analysis of the expression of all seven isoforms in five human pancreatic cancer cell lines by quantitative PCR and immunoblotting revealed that all seven isoforms were expressed in all the cell lines at both mRNA (Fig. 1B) and protein (Fig. 1C) levels. Moreover, high levels of 14-3-3σ mRNA were evident in BxPC3 and T3M4 cells, intermediate levels were present in ASPC-1 and COLO-357 cells, and low levels were present in PANC-1 cells. BxPC3 and T3M4 cells, which expressed high levels of 14-3-3σ mRNA, also exhibited high levels of 14-3-3σ protein in both cell lysates and conditioned medium (Fig. 1C and D). COLO-357 cells, which expressed intermediate levels of 14-3-3σ mRNA, exhibited high intracellular levels of 14-3-3σ protein but low levels of the protein in the medium, implying that the high intracellular levels were due in part to attenuated release of 14-3-3σ protein. ASPC-1 and PANC-1 cells, which expressed low levels of 14-3-3σ mRNA, also expressed low levels of the protein. Furthermore, PANC-1 cells released low levels of 14-3-3σ into conditioned medium, whereas ASPC-1 cells did not release detectable levels of 14-3-3σ. This failure to release 14-3-3σ may explain why ASPC-1 cells exhibited higher levels of intracellular 14-3-3σ than PANC-1 cells. To confirm that the presence of 14-3-3σ protein in the medium was not simply due to its release from dead cells, the membrane was blotted for tubulin, a cytoplasmic protein. Tubulin was detected only in the whole-cell lysates and not in the medium from any of the cell lines (Fig. 1D).

The protein levels of 14-3-3θ were highest in PANC-1 cells and lowest in BxPC3 cells, and the levels of 14-3-3γ were highest in T3M4 cells and lowest in ASPC-1 cells (Fig. 1C). The protein levels for the remaining isoforms were relatively uniform in all five cell lines.

***Effects of 14-3-3σ overexpression in PANC-1 cells on cisplatinum-induced apoptosis.*** In view of the fact that PANC-1 cells

expressed low level of 14-3-3σ protein, we reasoned that this cell line would be useful for assessing the biological role of 14-3-3σ in pancreatic cancer. Accordingly, we generated PANC-1 clones (C1 and C7) that overexpressed 14-3-3σ (Fig. 2A). 14-3-3σ levels in the clones C1 and C7 were comparable with the endogenous expression levels in BxPC3 and COLO-357 cells and were much higher than the endogenous levels in PANC-1 cells (Fig. 2B). Overexpression of 14-3-3σ was also associated with its increased release into conditioned medium (Fig. 2C). Following a more prolonged exposure of the membrane, a faint band corresponding to 14-3-3σ was seen in conditioned medium from sham-transfected cells (data not shown), in agreement with the observation that PANC-1 cells express low levels of endogenous 14-3-3σ (Fig. 1C). By immunofluorescence using an anti-14-3-3σ antibody, the overexpressed protein localized to both the cytoplasm and the perinuclear region (Fig. 2D). Similar results were observed with the anti-HA antibody (data not shown).

To determine whether high levels of 14-3-3σ modulate apoptotic signaling, the effects of cisplatinum on PARP cleavage and caspase-3 activation were examined. In response to 10 μg/mL cisplatinum, both 14-3-3σ-overexpressing clones exhibited

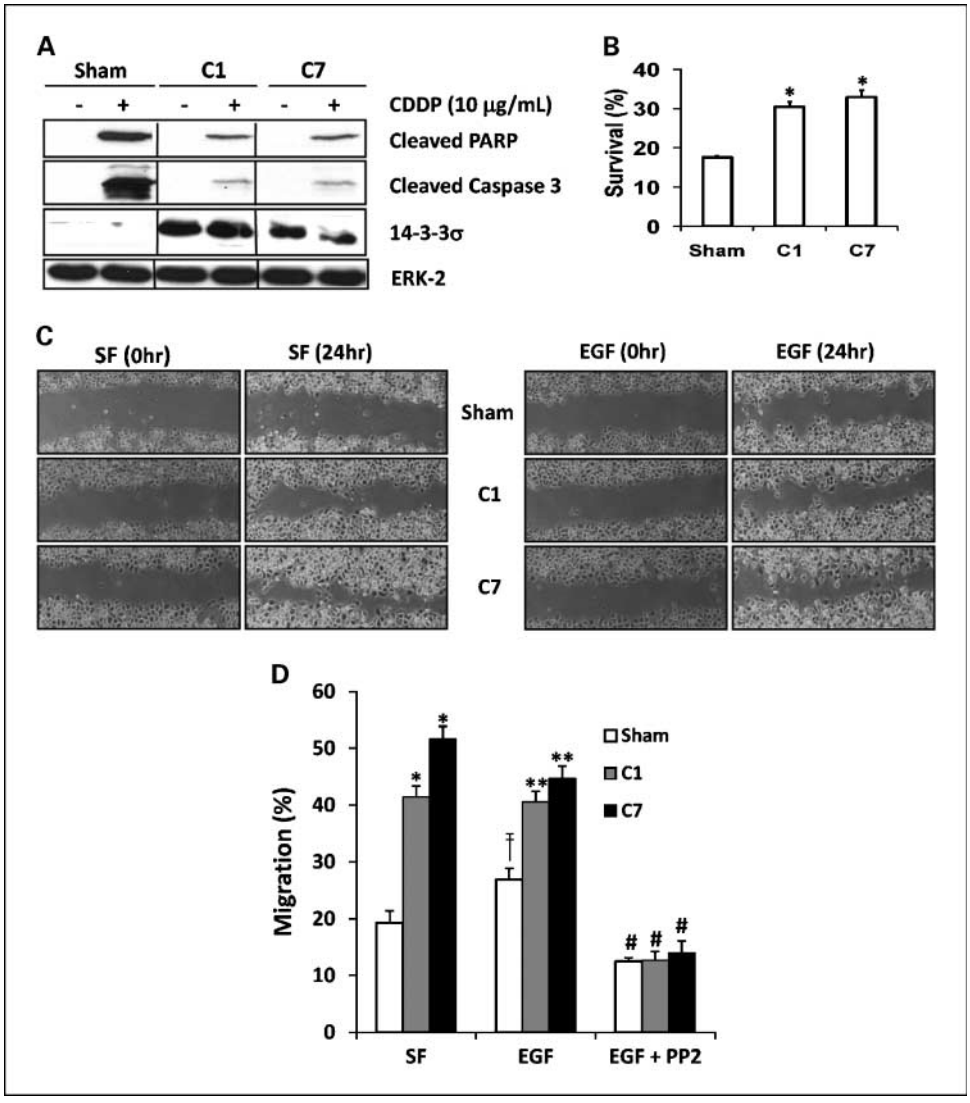


**Fig. 3.** Effects of 14-3-3σ overexpression in PANC-1 cell apoptosis and motility. *A,* effect of 14-3-3σ on cisplatinum-induced apoptosis. Apoptosis was assessed by monitoring PARP cleavage and caspase-3 activation after a 24 h incubation of sham-transfected and 14-3-3σ-expressing clones (C1 and C7) with 10 μg/mL cisplatinum (CDDP). Cell lysates (20 μg/lane) were subjected to immunoblotting with anti-cleaved PARP and anti-cleaved caspase-3 antibodies. Membrane was also probed with the anti-14-3-3σ antibody to confirm its expression in C1 and C7 and with the anti-ERK-2 antibody to verify equal loading of lanes. The protein lysates were all run on the same SDS-PAGE gel, but the lanes from each group were scanned separately (*vertical lines*). *B,* effect of 14-3-3σ on survival. Sham-transfected and 14-3-3σ-expressing clones (C1 and C7) were incubated for 48 h with 10 μg/mL cisplatinum. 3-(4,5-Dimethylthiazol-2-yl)-2,5-diphenyltetrazolium bromide assays were done as described in Materials and Methods. Mean ± SE of three independent experiments done with 6 wells per sample. *, $P < 0.01$, compared with Sham. *C,* wound-healing assays. Sham-transfected and 14-3-3σ-expressing clones (C1 and C7) were incubated in serum-free (*SF*) conditions in the absence or presence of EGF (1 nmol/L) for 24 h after making the scratch (wound). Representative pictures of wound-healing assays that were done to assess the motility of PANC-1 cells as described in Materials and Methods. Magnification, ×40. *D,* quantitative analysis of the images and effects of the Src kinase inhibitor PP2 on motility. Sham-transfected and 14-3-3σ-expressing clones C1 and C7 were incubated in the absence (*SF*) or presence of the indicated additions. SF, serum-free medium only; EGF, 1 nmol/L EGF added to serum-free medium; EGF + PP2, 1 nmol/L EGF and 10 μmol/L PP2 added to serum-free medium. Mean ± SE of three independent experiments. Data were analyzed by one-way ANOVA followed by Tukey HSD. *, $P < 0.05$, compared with sham serum-free medium; ‡, $P < 0.01$, compared with sham serum-free medium; **, $P < 0.01$, compared with sham EGF; #, $P < 0.05$, compared with respective serum-free or EGF treatment.

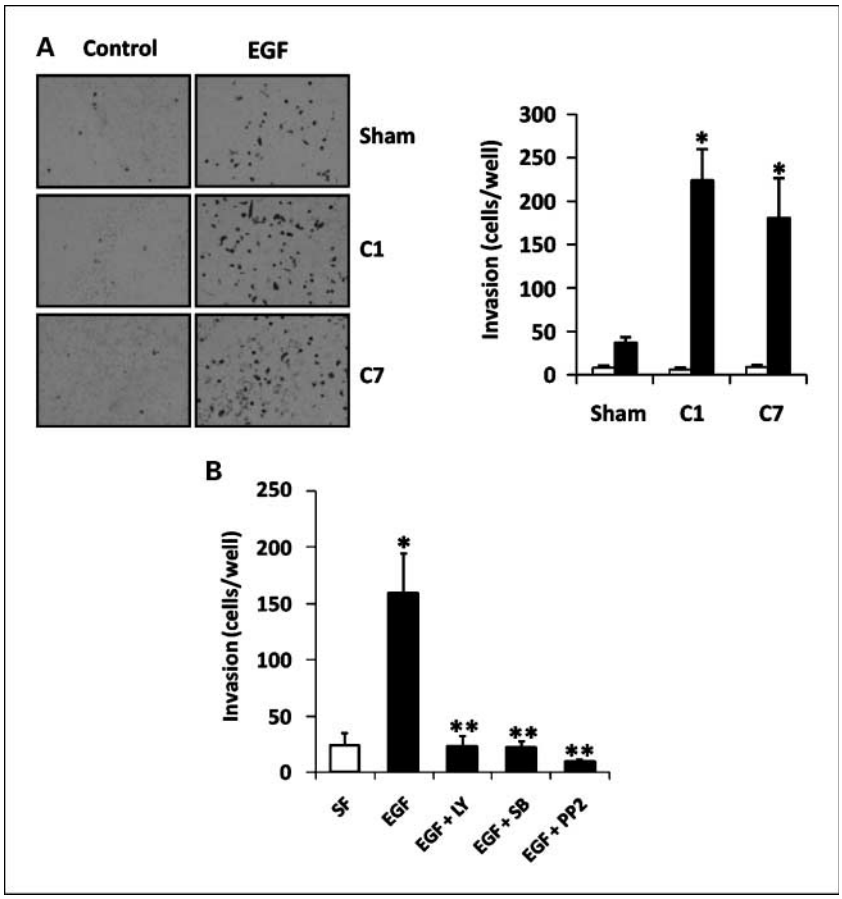


**Fig. 4.** Effects of 14-3-3σ on EGF-stimulated invasion. *A,* sham-transfected and 14-3-3σ-expressing clones (C1 and C7) were plated ($3 \times 10^4$ cells per well) on the top wells of Matrigel chambers and incubated in the absence (□) or presence (■) of EGF (1 nmol/L) in the lower compartment as chemoattractant for 20 h. Cells that had invaded through the Matrigel layer were fixed and stained as described in Materials and Methods. Representative pictures of membranes containing invading cells (*left*). Magnification, ×200. Quantification of the effects of EGF on invasion of sham-transfected and 14-3-3σ-expressing clones (C1 and C7; *right*). The number of invading cells in each membrane was counted using an inverted microscope (magnification, ×200) after staining with toluidine blue. Mean ± SE of duplicate determinations from three independent experiments. *, $P < 0.01$, compared with the EGF-treated sham. *B,* effects of inhibiting phosphatidylinositol 3-kinase, p38 mitogen-activated protein kinase, and Src kinase on EGF-induced invasion in 14-3-3σ-overexpressing cells (clone C1). Cells were incubated for 20 h in the absence or presence of EGF (1 nmol/L) alone or EGF together with LY294002 (5 μmol/L), SB203580 (10 μmol/L), or PP2 (10 μmol/L). Mean ± SE of duplicate determinations from three independent experiments. *, $P < 0.01$, compared with control values in the absence of EGF; **, $P < 0.01$, compared with EGF stimulation in the absence of any of the inhibitors.

attenuated PARP cleavage and markedly decreased generation of cleaved caspase-3, which is the activated form of caspase-3, by comparison with the effects seen in the sham-transfected PANC-1 cells (Fig. 3A). This decrease in cisplatinum-induced apoptosis was associated with a significant ($P < 0.01$) increase in the survival of these clone as determined with a 3-(4,5-dimethylthiazol-2-yl)-2,5-diphenyltetrazolium bromide assay (Fig. 3B).

***Effects of 14-3-3σ overexpression on motility and invasion in PANC-1 cells.*** To determine whether high levels of 14-3-3σ were associated with alteration in migration and invasion properties, migration and invasion assays were done next. Given the importance of the EGFR in the aggressiveness of pancreatic cancer and its known capacity for stimulating cell migration and invasion (3), the effects of EGF on motility were also studied.

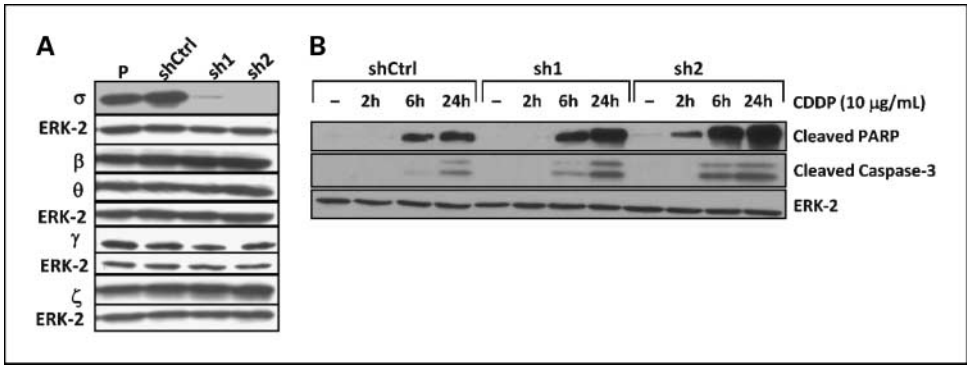


**Fig. 5.** Effects of silencing 14-3-3σ on apoptosis in T3M4 cells. *A,* whole-cell protein lysates from T3M4 parental cells (*P*) or cells infected with either a control shRNA (shCtrl) or a 14-3-3σ-specific shRNA (sh1 or sh2) were subjected to immunoblotting 72 h after infection with the lentivirus (multiplicity of infection of 40). The levels of all 14-3-3 proteins were assessed by immunoblotting with isoform-specific antibody to ensure the specificity of the shRNA against 14-3-3σ. Knockdown of 14-3-3σ protein was routinely monitored during the entire period of the subsequent experiments. *B,* effect of 14-3-3σ knockdown in cisplatinum-induced apoptosis. T3M4 cells infected with either a control shRNA (shCtrl) or 14-3-3σ specific shRNA (sh1 or sh2) were incubated in complete medium for 24 h that was supplemented with 10 μg/mL cisplatinum (CDDP) for the initial 2 or 6 h or the entire 24 h. After treatment, both floating and adherent cells were lysed and probed for PARP and caspase-3 cleavage as described in Materials and Methods. Two bands seen in the cleaved caspase-3 panel are 17 and 19 kDa fragments of activated caspase-3. Blots were probed for ERK-2 to ensure equal protein loading.

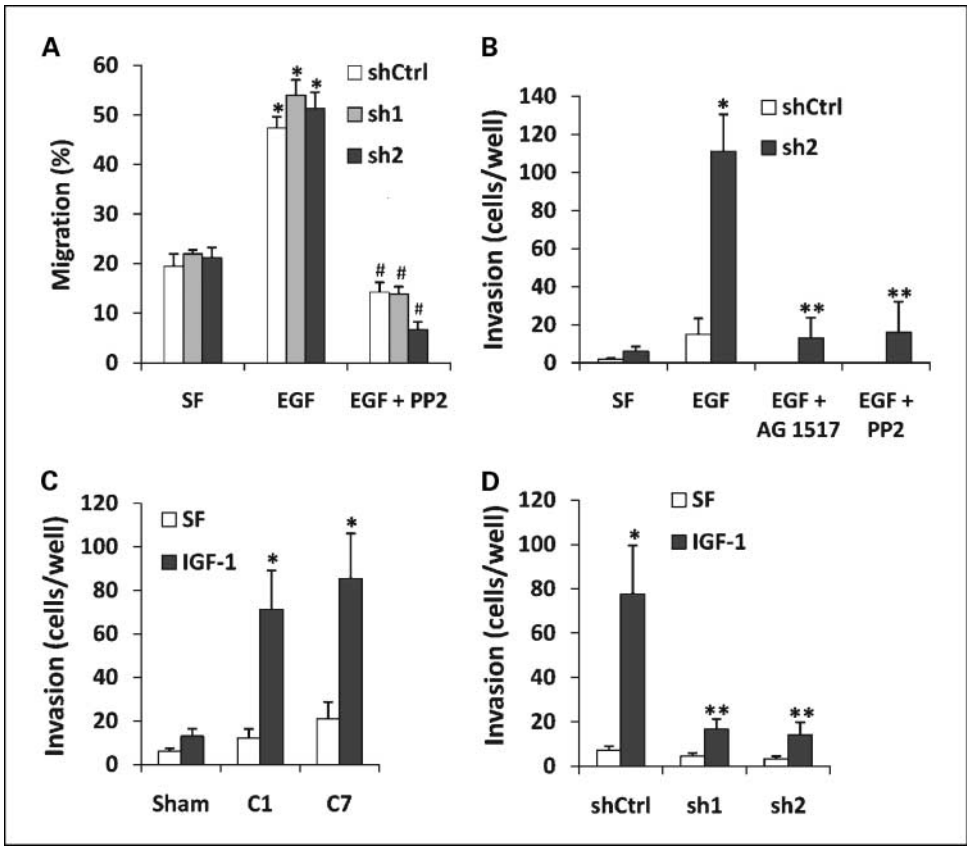


**Fig. 6.** Effects of silencing 14-3-3σ on motility and invasion in T3M4 cells. *A,* wound-healing assays in 14-3-3σ-silenced T3M4 cells. Control shRNA (shCtrl) or 14-3-3σ-specific shRNA (sh1 or sh2) infected cells were subjected to wound-healing assay in the absence or presence of EGF (1 nmol/L) with or without Src kinase inhibitor PP2 (10 μmol/L) for 24 h as described in Materials and Methods. Mean ± SE of three independent experiments. *, $P < 0.01$, compared with respective serum-free conditions; #, $P < 0.01$, compared with respective EGF treatment. *B,* Matrigel invasion assays. Control shRNA (shCtrl) or 14-3-3σ-specific shRNA (sh2) infected cells ($5 \times 10^4$ per well) were subjected to Matrigel invasion assay in the absence or presence of EGF (1 nmol/L) for 18 h. For inhibition studies, sh2-infected cells were incubated in Matrigel chambers in either the absence or the presence of EGF (1 nmol/L) together with AG1517 (1 μmol/L) or PP2 (10 μmol/L). Mean ± SE of duplicate determinations from three independent experiments. *, $P < 0.01$, compared with EGF in shCtrl; **, $P < 0.01$, compared with EGF in sh2. *C,* effects of 14-3-3σ overexpression on IGF-I-stimulated invasion. Sham-transfected and 14-3-3σ-expressing clones C1 and C7 ($3 \times 10^4$ cells per well) were plated on the upper wells of Matrigel chambers and incubated in the absence (SF) or presence of IGF-I (1 nmol/L) in the lower compartment as chemoattractant for 20 h. Cells that had invaded through the Matrigel layer were fixed and stained as described in Materials and Methods. Mean ± SE of duplicate determinations from three independent experiments. *, $P < 0.01$, compared with IGF-I-treated Sham. *D,* effects of silencing 14-3-3σ on IGF-I-stimulated invasion. Control shRNA (shCtrl) or 14-3-3σ-specific shRNA (sh1 or sh2) infected cells ($5 \times 10^4$ per well) were subjected to invasion assay in the absence (SF) or presence of IGF-I (1 nmol/L) as chemoattractant for 18 h. Mean ± SE of duplicate determinations from three independent experiments. *, $P < 0.01$, compared with shCtrl serum-free medium; **, $P < 0.01$, compared with IGF-I-treated shCtrl.

14-3-3σ-overexpressing clones were twice as motile as sham cells (Fig. 3C and D). EGF caused a slight but significant increase in the motility of sham-transfected cells (Fig. 3D) but did not cause an additional increase in motility in 14-3-3σ-overexpressing cells (Fig. 3D). The Src kinase inhibitor PP2 significantly attenuated basal (data not shown), EGF-stimulated (Fig. 3D), and 14-3-3σ enhanced motility (Fig. 3D). By contrast, although there was a trend for EGF to enhance the invasion of sham-transfected cells, this effect was not statistically significant, whereas EGF markedly enhanced the invasion of 14-3-3σ-overexpressing clones (Fig. 4A). LY294002, a phosphatidylinositol 3-kinase inhibitor, SB203580, a p38 mitogen-activated protein kinase inhibitor, and PP2, the Src kinase inhibitor, all suppressed EGF-mediated invasion in 14-3-3σ-overexpressing clones (Fig. 4B).

***Effects of 14-3-3σ on cisplatinum-induced apoptosis, cell motility, and invasion in T3M4 cells.*** To determine whether silencing endogenously high levels of 14-3-3σ would make pancreatic cancer cells more sensitive toward cisplatinum, the lentiviral shRNA approach was used to down-regulate 14-3-3σ gene in T3M4 cells, which have high endogenous levels of 14-3-3σ. Two different shRNA sequences (sh1 and sh2) targeting 14-3-3σ were determined to reduce 14-3-3σ levels, with sh2-mediated knockdown being more effective than sh1 (Fig. 5A). By contrast, the scrambled control shRNA (shCtrl) did not alter 14-3-3σ protein levels (Fig. 5A), and the shRNA specific to 14-3-3σ had no effect on the mRNA and protein levels of other members of 14-3-3 family (Fig. 5A; data not shown).

Next, T3M4 cells infected with either control or specific shRNA were incubated with cisplatinum (10 μg/mL) for 2, 6, or 24 h, and apoptosis was assessed by immunoblotting for cleaved PARP and cleaved caspase-3. Cells with silenced 14-3-3σ exhibited increased apoptosis compared with nonsilenced cells as evidenced by increased PARP cleavage and caspase-3 activation (Fig. 5B). Cells infected with sh2, which was better at silencing 14-3-3σ compared with sh1, were relatively more sensitive to cisplatinum as evidenced by higher levels of PARP cleavage and caspase-3 activation, and both were significantly more sensitive than control cells (Fig. 5B).

Silencing of 14-3-3σ did not lead to alterations in basal or EGF-stimulated motility in T3M4 cells. Thus, cells infected with control shRNA and specific shRNA (sh1 or sh2) were equally motile (20%), and EGF stimulated the motility to ~50% in all three groups (Fig. 6A). The EGF-stimulated increase in motility was abrogated by Src kinase inhibitor PP2. EGF induced a marked increase in invasion in 14-3-3σ down-regulated cells (sh2 infected) compared with invasion in control shRNA-infected cells, and this stimulatory effect was suppressed by AG1517 (1 μmol/L), an EGFR kinase inhibitor, and by PP2, a Src kinase inhibitor (Fig. 6B).

***Effects of 14-3-3σ levels on IGF-I-stimulated invasion.*** In view of the divergent effects of 14-3-3σ levels in PANC-1 and T3M4 cells in relation to EGF-mediated cell invasion, we next examined the effects of IGF-I on cell invasion in both cell lines. IGF-I significantly increased the invasion of PANC-1 clones overexpressing 14-3-3σ compared with its effect in sham cells (Fig. 6C). Conversely, the effects of IGF-I on invasion were markedly attenuated in T3M4 cells in which 14-3-3σ was silenced (Fig. 6D).

## Discussion

Several lines of evidence suggest that 14-3-3σ may function as a tumor suppressor gene. First, 14-3-3σ is the only member of the 14-3-3 family that is induced following DNA damage (25) and is required to prevent mitotic catastrophe following such damage (26). Second, the ectopic expression of 14-3-3σ leads to a $G_2$ arrest (27) due to the sequestration of CDC2-cyclin B1 in the cytoplasm (26). Third, 14-3-3σ is silenced or underexpressed in breast (10), prostate (28), and hepatic cancers (11). In these cases, there is strong evidence for epigenetic inactivation, which occurs as a consequence of hypermethylation at the gene locus (10, 11, 29). Additional mechanisms for the down-regulation of 14-3-3σ levels include mutations or functional deregulation of p53, which is known to directly induce 14-3-3σ expression (27), and E3 ubiquitin ligase-mediated degradation of 14-3-3σ (30). Although the p53 gene is frequently mutated in PDAC, 14-3-3σ is overexpressed in this cancer (12–15). In the cell lines investigated in this study, only COLO-357 cells have wild-type p53, whereas the other four cell lines have nonfunctional p53 (31, 32). There was no correlation between p53 gene status on 14-3-3σ levels (data not shown). Although the mechanisms underlying overexpression of 14-3-3σ in PDAC are not known, in contrast to several cancers where the 14-3-3σ gene is silenced by hypermethylation, the 14-3-3σ gene is hypomethylated in PDAC (33).

The 14-3-3 family proteins regulate diverse cellular processes often by binding to phosphorylated sites in many target proteins (6). Recently, 14-3-3σ was shown to preferentially form homodimer and this structural feature may be responsible for its unique role in response to DNA damage and human oncogenesis (34). In addition, 14-3-3σ exerts antiapoptotic actions, in part, due to its ability to sequester proapoptotic proteins such as BAD and BAX (25, 35, 36). Thus, phosphorylation-dependent association of BAD and phosphorylation-independent association of BAX with 14-3-3σ prevents them from translocating to the mitochondria and activating the downstream apoptotic cascade.

In the present study, using laser capture samples, we showed that among all the members of the 14-3-3 family, only 14-3-3σ is overexpressed in the pancreatic cancer cells. Furthermore, we carried out a comparison of the expression levels of all 14-3-3 family members in several pancreatic cancer cell lines and determined that 14-3-3σ protein levels were relatively high in BxPC3, COLO-357, and T3M4 and relatively low in PANC-1 and ASPC-1 cells. This relative expression pattern for 14-3-3σ is in agreement with a previous report detailing 14-3-3σ expression in pancreatic cancer cells (31).

Given that PANC-1 cells expressed relatively low levels of endogenous 14-3-3σ at both mRNA and protein levels, we overexpressed 14-3-3σ in these cells by stable transfection, thereby achieving levels comparable with those observed in COLO-357 and BxPC3 cells. The overexpression of 14-3-3σ did not have a significant effect on cell cycle distribution (data not shown), indicating that in these cells high level of 14-3-3σ does not cause a $G_2$-M cell cycle arrest. However, 14-3-3σ-overexpressing clones exhibited increased resistance toward cisplatinum-induced apoptosis as evidenced by increased cell survival of the transfected clones in conjunction with a decrease in caspase-3 activation and PARP cleavage in response to cisplatinum by comparison with effects observed in sham-transfected cells. Furthermore, silencing 14-3-3σ in T3M4 cells, which have high endogenous levels of this protein, sensitized these cells to cisplatinum treatment. These observations suggest that the high levels of 14-3-3σ contribute to the mechanisms that induce chemoresistance to cisplatinum in pancreatic cancer and attenuate the proapoptotic signaling pathway in these cells. Several lines of evidence support this conclusion. Thus, increased 14-3-3σ was detected in drug-resistant human PDAC cell lines (37); deletion of 14-3-3σ was shown to sensitize colorectal cancer cells to doxorubicin-induced apoptosis (26); 14-3-3σ has been identified as one of the proteins responsible for the doxorubicin resistance in the breast cancer cell line MCF-7/AdVp3000 (38); overexpression of 14-3-3σ in HEK293 cells enhanced resistance toward mitoxantrone (38). Taken together with our current findings, these observations suggest that silencing or disrupting 14-3-3σ function may sensitize pancreatic cancer cells to drug-induced apoptosis.

One of the hallmarks of PDAC is the ability of pancreatic cancer cells to invade and metastasize (39–41). The EGFR has been implicated as having an important role in many cancers, where it acts to enhance proliferation, motility, invasiveness, metastasis, and chemoresistance (42, 43). Cultured human pancreatic cancer cell lines and human PDAC frequently express relatively high levels of the EGFR as well as the related receptors ErbB-2/HER2 and ErbB-3/HER3 (3). Moreover, EGF and related ligands, such as transforming growth factor-α, heparin-binding EGF-like growth factor, and amphiregulin enhance the proliferation and/or invasiveness of these cells (3, 44), indicating that the EGFR participates in many aberrant autocrine and paracrine loops that may contribute to the biological aggressiveness of PDAC. Indeed, the concomitant presence of the EGFR and either EGF or transforming growth factor-α is associated with enhanced tumor aggressiveness and shorter postoperative survival periods (45). In this context, our present finding that high levels of 14-3-3σ were associated with increased basal motility and a dramatic increase in EGF-stimulated invasiveness in PANC-1 cells raises the possibility that the concomitant overexpression of the EGFR and 14-3-3σ may greatly enhance the invasive capacity of pancreatic cancer cells *in vivo*. However, in T3M4 cells, silencing of 14-3-3σ was

not associated with a change in motility and led to increased EGF-stimulated cell invasion. By contrast, in the same cells, IGF-I-mediated invasion was robust in the presence of endogenously high levels of 14-3-3σ, and this effect was completely suppressed following 14-3-3σ silencing. Taken together, these observations indicate that the role of 14-3-3σ with respect to motility and invasion is cell type and context specific. In view of the important role of EGF in pancreatic cancer, these observations suggest that the concomitant targeting of EGFR and 14-3-3σ may be of therapeutic benefit in PDAC.

In the present study, we also determined that the EGF-mediated increase in invasiveness was completely blocked by LY294002, a phosphatidylinositol 3-kinase inhibitor, by SB203580, a p38 mitogen-activated protein kinase inhibitor, and by PP2, a Src kinase inhibitor. These findings suggest that, in the presence of high levels of 14-3-3σ, the phosphatidylinositol 3-kinase, p38 mitogen-activated protein kinase, and Src pathways contribute to this effect. Both phosphatidylinositol 3-kinase and p38 mitogen-activated protein kinase are activated by Src kinase on EGFR activation (46), and down-regulation of Src by small interfering RNA-mediated silencing or inhibition of Src kinase activity attenuate pancreatic tumor progression and metastasis in nude mice (47). In view of the known ability of 14-3-3σ to act as an adapter protein for signal transduction, our findings raise the possibility that, in some pancreatic cancer cells, 14-3-3σ promotes more efficient interactions between EGFR and Src kinase, leading to the marked increase in EGF-mediated invasiveness.

The three pancreatic cancer cell lines that exhibited high levels of intracellular 14-3-3σ also secreted 14-3-3σ into the medium. Moreover, engineered overexpression of 14-3-3σ in PANC-1 cells was accompanied by a parallel increase in 14-3-3σ secretion from these cells. To our knowledge, this is the first report that documents the secretion of 14-3-3σ by any cancer cells. Several lines of evidence indicate that the release of 14-3-3σ by the pancreatic cancer cells into the conditioned medium was not a spurious event caused by cell death. First, there was differential release of 14-3-3σ by the cells. Thus, detectable levels of 14-3-3σ were not observed in the medium from ASPC-1 cells in spite of the fact that they expressed 14-3-3σ, and only low levels of 14-3-3σ were present in the medium from COLO-357 cells in spite of its marked abundance in these cells. Moreover, PANC-1 cells, which expressed the lowest levels of 14-3-3σ in cell lysates, exhibited similar levels in the medium as observed in medium from COLO-357 cells, in spite of the known resistance of PANC-1 cells to apoptosis and anoikis. Second, under the experimental conditions used in the present study, the cells were viable by morphologic criteria and, whenever tested, by trypan blue exclusion. Third, tubulin, a cytoplasmic marker, was not detectable in the medium by Western blotting, indicating that cytoplasmic proteins were not being released into the medium in a nonspecific manner.

Previously, it has been reported that 14-3-3σ is secreted by differentiated keratinocytes and, that following release, 14-3-3σ induces matrix metalloproteinase-1 expression in dermal fibroblasts in a coculture system (48, 49). Moreover, treatment of fibroblasts with exogenous recombinant 14-3-3σ leads to increased matrix metalloproteinase-1 and -3 expression by fibroblasts. In view of the ability of matrix metalloproteinase-1 to degrade fibrillar collagen and matrix metalloproteinase-3 to promote carcinogenesis, these observations suggest that secreted 14-3-3σ may have an important role within the tumor microenvironment that may enhance cancer progression and raise the possibility that it may serve as a serum marker for those pancreatic cancers that express it at high levels.

In conclusion, 14-3-3σ was the most abundant isoform in the human cancer samples, and was readily secreted by most of the cancer cell lines. In both PANC-1 and T3M4 cells, 14-3-3σ conferred apoptosis resistance. In PANC-1 cells, 14-3-3σ promoted basal motility and enhanced EGF-mediated invasion, whereas in T3M4 14-3-3σ did not alter basal invasion but appeared to suppress EGF-mediated invasion while promoting IGF-I-mediated invasion. These observations indicate that 14-3-3σ could be a therapeutic target in PDAC especially when used in conjunction with EGFR targeted therapy, and raise the possibility that its presence in serum could serve as a diagnostic marker, or as an indicator of disease recurrence.

## Disclosure of Potential Conflicts of Interest

No potential conflicts of interest were disclosed.

## References


1. Jemal A, Siegel R, Ward E, et al. Cancer statistics, 2008. CA Cancer J Clin 2008;58:71–96.
2. Bardeesy N, DePinho RA. Pancreatic cancer biology and genetics. Nat Rev Cancer 2002;2:897–909.
3. Korc M. Role of growth factors in pancreatic cancer. Surg Oncol Clin N Am 1998;7:25–41.
4. Westphal S, Kalthoff H. Apoptosis: targets in pancreatic cancer. Mol Cancer 2003;2:6.
5. Arnold NB, Ketterer K, Kleeff J, Friess H, Buchler MW, Korc M. Thioredoxin is downstream of Smad7 in a pathway that promotes growth and suppresses cisplatin-induced apoptosis in pancreatic cancer. Cancer Res 2004;64:3599–606.
6. Fu H, Subramanian RR, Masters SC. 14-3-3 proteins: structure, function, and regulation. Annu Rev Pharmacol Toxicol 2000;40:617–47.
7. Rubio MP, Geraghty KM, Wong BH, et al. 14-3-3-affinity purification of over 200 human phosphoproteins reveals new links to regulation of cellular metabolism, proliferation and trafficking. Biochem J 2004;379:395–408.
8. Muslin AJ, Tanner JW, Allen PM, Shaw AS. Interaction of 14-3-3 with signaling proteins is mediated by the recognition of phosphoserine. Cell 1996;84:889–97.
9. Hermeking H. The 14-3-3 cancer connection. Nat Rev Cancer 2003;3:931–43.
10. Ferguson AT, Evron E, Umbricht CB, et al. High frequency of hypermethylation at the 14-3-3σ locus leads to gene silencing in breast cancer. Proc Natl Acad Sci U S A 2000;97:6049–54.
11. Iwata N, Yamamoto H, Sasaki S, et al. Frequent hypermethylation of CpG islands and loss of expression of the 14-3-3σ gene in human hepatocellular carcinoma. Oncogene 2000;19:5298–302.
12. Friess H, Ding J, Kleeff J, et al. Microarray-based identification of differentially expressed growth- and metastasis-associated genes in pancreatic cancer. Cell Mol Life Sci 2003;60:1180–99.
13. Logsdon CD, Simeone DM, Binkley C, et al. Molecular profiling of pancreatic adenocarcinoma and chronic pancreatitis identifies multiple genes differentially regulated in pancreatic cancer. Cancer Res 2003;63:2649–57.
14. Nakamura T, Furukawa Y, Nakagawa H, et al. Genome-wide cDNA microarray analysis of gene expression profiles in pancreatic cancers using populations of tumor cells and normal ductal epithelial cells selected for purity by laser microdissection. Oncogene 2004;23:2385–400.
15. Iacobuzio-Donahue CA, Ashfaq R, Maitra A, et al. Highly expressed genes in pancreatic ductal adenocarcinomas: a comprehensive characterization and comparison of the transcription profiles obtained from three major technologies. Cancer Res 2003;63:8614–22.
16. Perathoner A, Pirkebner D, Brandacher G, et al. 14-3-3σ expression is an independent prognostic parameter for poor survival in colorectal carcinoma patients. Clin Cancer Res 2005;11:3274–9.
17. Villaret DB, Wang T, Dillon D, et al. Identification of genes overexpressed in head and neck squamous cell carcinoma using a combination of complementary

DNA subtraction and microarray analysis. Laryngoscope 2000;110:374–81.

**18.** Kleeff J, Korc M. Up-regulation of transforming growth factor (TGF)-β receptors by TGF-β1 in COLO-357 cells. J Biol Chem 1998;273:7495–500.

**19.** Ketterer K, Rao S, Friess H, Weiss J, Buchler MW, Korc M. Reverse transcription-PCR analysis of laser-captured cells points to potential paracrine and autocrine actions of neurotrophins in pancreatic cancer. Clin Cancer Res 2003;9:5127–36.

**20.** Chomczynski P, Sacchi N. Single-step method of RNA isolation by acid guanidinium thiocyanate-phenol-chloroform extraction. Anal Biochem 1987;162:156–9.

**21.** Yasutome M, Gunn J, Korc M. Restoration of Smad4 in BxPC3 pancreatic cancer cells attenuates proliferation without altering angiogenesis. Clin Exp Metastasis 2005;22:461–73.

**22.** Raitano AB, Korc M. Tumor necrosis factor up-regulates γ-interferon binding in a human carcinoma cell line. J Biol Chem 1990;265:10466–72.

**23.** Baldwin RL, Korc M. Growth inhibition of human pancreatic carcinoma cells by transforming growth factor β-1. Growth Factors 1993;8:23–34.

**24.** Rowland-Goldsmith MA, Maruyama H, Kusama T, Ralli S, Korc M. Soluble type II transforming growth factor-β (TGF-β) receptor inhibits TGF-β signaling in COLO-357 pancreatic cancer cells *in vitro* and attenuates tumor formation. Clin Cancer Res 2001;7:2931–40.

**25.** Samuel T, Weber HO, Rauch P, et al. The $G_2$/M regulator 14-3-3σ prevents apoptosis through sequestration of Bax. J Biol Chem 2001;276:45201–6.

**26.** Chan TA, Hermeking H, Lengauer C, Kinzler KW, Vogelstein B. 14-3-3σ is required to prevent mitotic catastrophe after DNA damage. Nature 1999;401:616–20.

**27.** Hermeking H, Lengauer C, Polyak K, et al. 14-3-3σ is a p53-regulated inhibitor of $G_2$/M progression. Mol Cell 1997;1:3–11.

**28.** Cheng L, Pan CX, Zhang JT, et al. Loss of 14-3-3σ in prostate cancer and its precursors. Clin Cancer Res 2004;10:3064–8.

**29.** Lodygin D, Diebold J, Hermeking H. Prostate cancer is characterized by epigenetic silencing of 14-3-3σ expression. Oncogene 2004;23:9034–41.

**30.** Urano T, Saito T, Tsukui T, et al. Efp targets 14-3-3σ for proteolysis and promotes breast tumour growth. Nature 2002;417:871–5.

**31.** Guweidhi A, Kleeff J, Giese N, et al. Enhanced expression of 14-3-3σ in pancreatic cancer and its role in cell cycle regulation and apoptosis. Carcinogenesis 2004;25:1575–85.

**32.** Seki T, Ohba N, Makino R, Funatomi H, Mitamura K. Mechanism of growth-inhibitory effect of cisplatin on human pancreatic cancer cells and status of p53 gene. Anticancer Res 2001;21:1919–24.

**33.** Sato N, Maitra A, Fukushima N, et al. Frequent hypomethylation of multiple genes overexpressed in pancreatic ductal adenocarcinoma. Cancer Res 2003;63:4158–66.

**34.** Wilker EW, Grant RA, Artim SC, Yaffe MB. A structural basis for 14-3-3σ functional specificity. J Biol Chem 2005;280:18891–8.

**35.** Zha J, Harada H, Yang E, Jockel J, Korsmeyer SJ. Serine phosphorylation of death agonist BAD in response to survival factor results in binding to 14-3-3 not BCL-X(L). Cell 1996;87:619–28.

**36.** Nomura M, Shimizu S, Sugiyama T, et al. 14-3-3 interacts directly with and negatively regulates pro-apoptotic Bax. J Biol Chem 2003;278:2058–65.

**37.** Sinha P, Hutter G, Kottgen E, Dietel M, Schadendorf D, Lage H. Increased expression of epidermal fatty acid binding protein, cofilin, and 14-3-3σ (stratifin) detected by two-dimensional gel electrophoresis, mass spectrometry and microsequencing of drug-resistant human adenocarcinoma of the pancreas. Electrophoresis 1999;20:2952–60.

**38.** Liu Y, Liu H, Han B, Zhang JT. Identification of 14-3-3σ as a contributor to drug resistance in human breast cancer cells using functional proteomic analysis. Cancer Res 2006;66:3248–55.

**39.** Keleg S, Buchler P, Ludwig R, Buchler MW, Friess H. Invasion and metastasis in pancreatic cancer. Mol Cancer 2003;2:14.

**40.** Rowland-Goldsmith MA, Maruyama H, Matsuda K, et al. Soluble type II transforming growth factor-β receptor attenuates expression of metastasis-associated genes and suppresses pancreatic cancer cell metastasis. Mol Cancer Ther 2002;1:161–7.

**41.** Aikawa T, Whipple CA, Lopez ME, et al. Glypican-1 modulates the angiogenic and metastatic potential of human and mouse cancer cells. J Clin Invest 2008;118:89–99.

**42.** Ciardiello F, Tortora G. EGFR antagonists in cancer treatment. N Engl J Med 2008;358:1160–74.

**43.** Normanno N, Bianco C, De Luca A, Salomon DS. The role of EGF-related peptides in tumor growth. Front Biosci 2001;6:D685–707.

**44.** Li J, Kleeff J, Giese N, Buchler MW, Korc M, Friess H. Gefitinib ('Iressa', ZD1839), a selective epidermal growth factor receptor tyrosine kinase inhibitor, inhibits pancreatic cancer cell growth, invasion, and colony formation. Int J Oncol 2004;25:203–10.

**45.** Yamanaka Y, Friess H, Kobrin MS, Buchler M, Beger HG, Korc M. Coexpression of epidermal growth factor receptor and ligands in human pancreatic cancer is associated with enhanced tumor aggressiveness. Anticancer Res 1993;13:565–9.

**46.** Summy JM, Trevino JG, Baker CH, Gallick GE. c-Src regulates constitutive and EGF-mediated VEGF expression in pancreatic tumor cells through activation of phosphatidyl inositol-3 kinase and p38 MAPK. Pancreas 2005;31:263–74.

**47.** Trevino JG, Summy JM, Lesslie DP, et al. Inhibition of SRC expression and activity inhibits tumor progression and metastasis of human pancreatic adenocarcinoma cells in an orthotopic nude mouse model. Am J Pathol 2006;168:962–72.

**48.** Ghahary A, Karimi-Busheri F, Marcoux Y, et al. Keratinocyte-releasable stratifin functions as a potent collagenase-stimulating factor in fibroblasts. J Invest Dermatol 2004;122:1188–97.

**49.** Ghahary A, Marcoux Y, Karimi-Busheri F, et al. Differentiated keratinocyte-releasable stratifin (14-3-3σ) stimulates MMP-1 expression in dermal fibroblasts. J Invest Dermatol 2005;124:170–7.